Remarkable differences and similarities between the isomeric Mn(II)- cis - and trans- 1,2-diaminocyclohexane- N , N , N ', N '-tetraacetate complexes

Enikő Molnár, Balázs Váradi, Zoltán Garda, Richárd Botár, Ferenc Kálmán, Éva Tóth, Imre Toth, Ernő Brücher, Gyula Tircsó

Remarkable differences and similarities between the isomeric Mn(II)- *cis*- and *trans*-1,2-diamionocyclohexane-tetraacetate complexes

Enikő Molnár[a], *Balázs Váradi*[a], *Zoltán Garda*[a], *Richárd Botár*[a], *Ferenc K. Kálmán*[a], *Éva Tóth*[b], *Imre Tóth*[a], *Ernő Brücher*[a] *and Gyula Tircsó*[a*]

[a] Department of Inorganic and Analytical Chemistry, Faculty of Science and Technology, University of Debrecen, Debrecen, Egyetem tér 1, H-4010, Hungary

[b] Centre de Biophysique Moléculaire, CNRS, Université d'Orléans, rue Charles Sadron, 45071 Orléans, Cedex 2, France

This paper is dedicated to Prof. Imre Sóvágó on the occasion of his 70th birthday.

Corresponding author e-mail: gyula.tircso@science.unideb.hu

Keywords

Magnetic resonance Imaging (MRI), Contrast Agents (CAs), Manganese(II) complexes, Stability, Inertness, Solvent exchange, Relaxivity

Abstract

Equilibrium, kinetic (solvent exchange and dissociation of the complex) and relaxometric studies (^{1}H and ^{17}O NMR) have been performed with the [M(II)(*c*-cdta)]$^{2-}$ complexes (*c*-cdta = *cis*-1,2-diaminocyclohexane-*N,N,N′,N′*-tetraacetic acid, M(II)= Mn(II), Zn(II), Cu(II),Ca(II), Mg(II)) and the physico-chemical data are compared to the isomeric complexes with *trans*-1,2-cdta (*t*-cdta) with the aim of searching appropriate ligands for Mn(II) complexation for safe MRI contrast agents. The total basicity ($\Sigma \log K_5^H$) of the *c*-cdta ligand appears to be very similar to that of the *trans*- derivative under the conditions applied (I=0.15 M NaCl and 25 ^{o}C), but the first two protonation constants notably differ. $\log K_1^H$ is 1.5 log units higher, while the $\log K_2^H$ is 0.8 log units lower than those determined for the *trans*-derivative. Similar basicity of the ligands results in similar complex stability ($\log K_{[Mn(L)]}$ values are 14.19(2) and 14.32), whereas the conditional stabilities near to physiological pH are different (pMn values are 7.82 and 8.68) for the [Mn(*c*-cdta)]$^{2-}$ and the [Mn(*t*-cdta)]$^{2-}$ derivatives, respectively. Dissociation kinetic studies revealed that the [Mn(*c*-cdta)]$^{2-}$ dissociates 250 times faster than the [Mn(*t*-cdta)]$^{2-}$ complex. The water exchange rate (k_{ex}^{298}) of [Mn(*c*-cdta)]$^{2-}$ is ca. 60% higher than that of [Mn(*t*-cdta)]$^{2-}$. The differences can likely be attributed to the different distances between the individual donor atoms, and the arrangement of the donor atoms around the metal ions in the *cis*- and *trans*- isomers. Interestingly, the relaxivity values of the Mn(II) complexes are very close (r_{1p} = 3.85 $mM^{-1}s^{-1}$ and 3.62 $mM^{-1}s^{-1}$; 20 MHz, 25 °C for the *cis*- and *trans*-isomers, respectively). The results gained in our studies confirm, that the *trans*-1,2-cyclohexanediamine “building block” display better features for further ligand development.

Introduction

The linear and macrocyclic aminopolycarboxylate (APC) complexes are widely used in medical diagnosis and therapy for the complexation of metal ions applied in the field of nuclear medicine, optical and magnetic resonance imaging (MRI) [1-7]. These different fields

have some special claims regarding the properties of complexes, but the general requirements, what should be accomplished for all the complexes, are the high stability and kinetical inertness. In other words, it means that the complexes must not dissociate in the body of patients during and after the examinations are performed. Considering the very complex nature of biological fluids which contain a great number of metal ions and complex forming ligands, this is a very strict requirement. Preventing any interaction between the APC complexes in use and the endogenous metals or ligands, the structure of APC ligands play very important role. So the ligands have to be specially designed for the robust complexation of metal ions. To design a ligand, the chemical properties of metal ions, its ionic size, electronic structure and coordination number are considered first to find out how many and which kind of donor atoms are optimal for the complexation. Some special structural elements may also be beneficial e.g. the rigidity of the ligand and/or pre-organize it for the metal ion by the use of suitable functional group(s) and/or by introducing some cyclic or macrocyclic building blocks.

In MRI several Gd(III) – APC complexes are clinically used as contrast agents (CAs) to increase the contrast between the healthy and diseased tissues or organs by differently increasing the relaxation rates of protons (mainly water protons) in the body. The complex forming ligands used in the CAs are the linear dtpa, the macrocyclic dota and their derivates [6, 7]. Recently there are 6 linear and 3 macrocyclic CAs in clinical use but in the last decade some concerns arose with the use of the linear agents. It was recognized that a new disease, called nephrogenic systemic fibrosis (NSF), was associated with the use of the Gd^{3+}-based CAs. NSF was developed in patients with severe renal impairment, when the elimination of the CAs was slow and during the longer residence time of the Gd(III) complex in the body of patients a small amount of Gd(III) remained deposited, that presumably triggered the development of NSF [8-10]. More recently the presence of Gd has been detected in different organs, also in the brain of patients with normal renal function after a few repeated MR scans using CAs [11-14]. The presence of traces of non-chelated Gd(III) in the body of patients caused anxiety because the strong toxicity of Gd(III) ion. These problems with the use of the linear Gd(III)-based CAs turned the attention of researchers to the complexes of Mn(II) as potential contrast agents [15-16]. The relaxation effects of Mn(II) ion are known to be similar to that of Gd(III), but on the other hand, Mn(II) is an essential metal ion and some amount of the intravenously administered Mn(II) is eliminated relatively rapidly through the hepatobiliary system. Since the coordination number of Gd(III) is 8-9, while that of Mn(II) is

6-7, the ligands used in the Gd(III)-based CAs can not directly be used for the complexation of Mn(II). Some examples are known, when the Mn(II) complexes with ligands performing well with Gd(III) are stable and inert, but the absence of inner sphere water molecule(s) results in negligible enhance in the contrast) [17]. Another critical point is the lability/inertness of the complexes (the terms lability/inertness in this manuscript describe dissociation kinetics parameters of the complexes rather than the solvent exchange kinetics). The majority of the open-chain ligands form very labile complexes with the Mn(II). The most socking example is that of $[Mn(dtpa)]^{3-}$ which was found to dissociate within the dead-time of the stopped-flow instrument (ca. 8 msec) in the presence Cu(II) ion as a ligand scavenger [18]. In order to find suitable ligands for Mn(II), a number of new linear and macrocyclic ligands were synthesized during the last years and the properties of their complexes were investigated extensively [15-24]. Amongst the hexadentate linear ligands edta forms relatively stable $[Mn(edta)]^{2-}$ complex in which a water molecule occupies the seventh coordination site, but the kinetic inertness of the complex is also low, because of the flexible structure of the ligand [18]. The edta analogue *trans*-1,2-cdta (abbreviated as *t*-cdta through the text, Figure 1) ligand is more rigid and it forms more stable and more inert complex, $[Mn(t\text{-}cdta)]^{2-}$, than $[Mn(edta)]^{2-}$, therefore it seems to be suitable as a potential CA and recently was evaluated even in preclinical studies [25-26]. The behaviour of the cdta derivative ligands are likely similar to the parent ligand, so their Mn(II) complexes are promising for the preparation of Mn(II)-based MRI CAs [18, 22].

While the complexation properties of the *t*-cdta ligand have been studied extensively, there is very few knowledge about the complexes of the other stereoisomer, the *cis*-1,2-cdta ligand (abbreviated as *c*-cdta in the text). The donor atoms of the *t*-cdta form a semi-rigid preorganized coordination cage, where metal ions of different size may enter and generally form complexes of high stability [27]. The maximum distance between the two *N*-donor atoms in *t*-cdta is 4 Å, while that in the *c*-cdta is 3.1 Å only [28], so the coordination cage formed by the donor atoms of *cis*- isomer is relatively small, particularly for larger metal ions, that predicts low stability complexes with *c*-cdta. Since the size of the Mn(II) ion is not too large and there are only very few data in the literature regarding the complexation of *c*-cdta, we decided to study its complexes with Mn(II) and with some other endogenous metal ions.

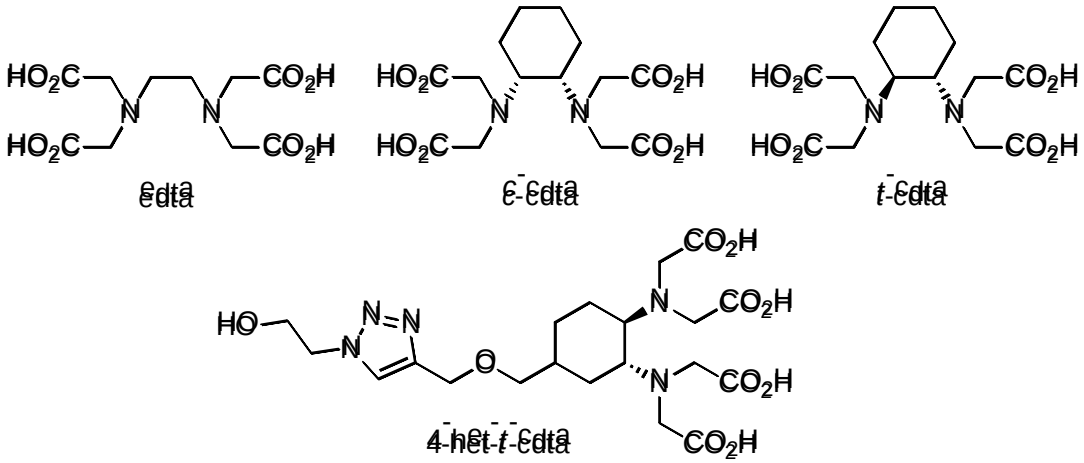

Figure 1. Formulae of the edta, *c*-cdta, *t*-cdta, 4-het-*t*-cdta ligands.

Results and Discussion

The synthesis of *c*-cdta ligand (Scheme 1) was accomplished in a two-step reaction sequence starting from *cis*-cyclohexane-1,2-diamine which was alkylated by using ethyl bromoacetate in the presence of Hünig's base (diisopropylethyl amine, dipea). The saponification of the tetraethyl ester with NaOH afforded the product which was purified by recrystallization form acidic (pH=2.0) aqueous solution.

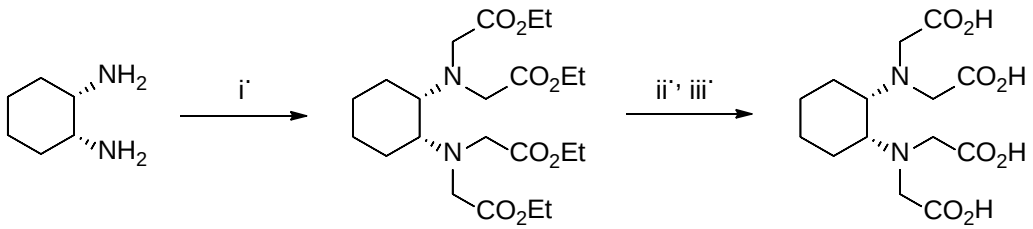

Scheme 1. The synthesis of the *c*-cdta chelator: i). 4.2 equivalent of ethyl bromoacetate, DIPEA, MeCN, 7 h reflux; ii). 6 equivalent of NaOH, EtOH, 24 h reflux; iii). cc HCl till pH = 2.0.

Equilibrium studies

In order to characterize the metal complexes as potential MRI contrast enhancement agents, we have to know their equilibrium and kinetic behaviour in biofluids, the proton relaxation effects, together with another parameters which determine the proton relaxation

rates in the presence of these complexes. For the assessment of the equilibrium behaviour we have determined the stability constant of the Mn(II) complex and those of the Mg(II), Ca(II), Zn(II) and Cu(II) complexes that may compete with the Mn(II) ion for the *c*-cdta ligand in biofluids. To obtain information about the kinetic inertness of $[Mn(c\text{-cdta})]^{2-}$ complex, the rates of the exchange reactions occurring between the complex and Cu(II) ion have been investigated, *vide infra*. These properties are already known for the $[Mn(t\text{-cdta})]^{2-}$ complex, so the comparison of the behaviour of the two complexes is possible.

The protonation constant of the *c*-cdta ligand have been determined by pH-potentiometric titration. The protonation constants (K_i^H) defined by Equation (1), are presented in Table 1.

$$K_i^H = \frac{[H_iL]}{[H_{i-1}L][H^+]} \qquad \text{where i=1, 2, n} \qquad \text{(eqn. 1)}$$

where i = 1, 2, …, 5, $[H_iL]$, $[H_{i-1}L]$ and $[H^+]$ are the equilibrium concentrations of the H_iL and $H_{i-1}L$ ligand species and the H^+ ions, respectively. The stability constants of the ML complexes (K_{ML}) are defined by Equation (2):

$$K_{ML} = \frac{[ML]}{[M][L]} \qquad \text{(eqn. 2)}$$

In Equation (2) [M], [ML] and [L] are the equilibrium concentrations of the M(II) metal ion, ML complex and L^{4-} ligand, respectively (the charges of ions will be used only when it is necessary).

The metal ions and protons compete for the ligand, so at lower pH values protonated complex can be formed. The protonation constant of complexes is defined as follows:

$$K_{MH_iL} = \frac{[MH_iL]}{[MH_{i-1}L][H^+]} \qquad \text{(eqn. 3)}$$

where i = 1 or 2, $[M(H_iL)]$ and $[M(H_{i-1}L)]$ are the concentration of the protonated complexes.

Table 1. Protonation constants of the *c*-cdta, *t*-cdta and and edta ligands and stability constants of their Mg(II), Ca(II), Zn(II), Cu(II) and Mn(II) complexes (log *K* values, 25°C, 0.15 NaCl).

		c-cdta[a]	*c*-cdta[b]	*t*-cdta[c]	*t*-cdta[b]	edta[c]
H^+	log K_1^H	**11.00(1)**	10.70	9.54	11.70	9.28
	log K_2^H	**5.20(1)**	5.21	5.97	6.12	6.04
	log K_3^H	**3.41(1)**	3.50	3.60	3.52	2.72
	log K_4^H	**2.30(1)**	2.44	2.52	2.43	1.99
	log K_5^H	**1.41(1)**	–	1.46	–	1.11
	$\sum \log K_i^H$	**23.32**	21.85	23.09	23.77	21.14
Mg^{2+}	log K_{ML}	**9.01(2)**	8.38	9.14	11.07	7.61
	log K_{MHL}	**4.72(6)**	4.44	3.53	–	–
Ca^{2+}	log K_{ML}	**9.65(2)**	9.45	10.23	13.15	9.53
	log K_{MHL}	**4.55(5)**	4.11	3.53	–	2.92
Mn^{2+}	log K_{MnL}	**14.19(2)**	–	14.32[d]	17.48	12.46[d]
	log K_{MnHL}	**2.85(3)**	–	2.90[d]	2.8	2.95[d]
	log K_{MnH2L}	–	–	1.89[d]	–	–[d]
	pMn[e]	**7.82**	–	8.68	–	7.83
Zn^{2+}	log K_{ML}	**17.06(1)**	–	16.75	19.37	15.92
	log K_{MHL}	**2.76(1)**	–	2.57	2.9	3.23
	log K_{MH2L}	–	–	–	–	1.50
Cu^{2+}	log K_{ML}	**18.3(1)[f]**	–	19.78[f]	22.0	19.02[f]
	log K_{MHL}	**3.65(3)**	–	2.91	3.1	3.15
	log K_{MH2L}	–	–	1.10	–	2.04

[a] this work; [b] Ref. [27]; [c] 0.15 M NaCl, 25°C from the diploma work of Veronika Józsa, 2015, University of Debrecen, Debrecen, Hungary; [d] Ref. [18]; [e] calculated by using $c_{Mn}=c_{Lig}=0.01$ mM at pH=7.4 according Tóth et al. [29]; [d] determined by simultaneous fitting of the UV-vis and pH-potentiometic data.

The protonation constants of *c*-cdta determined in this work at 25°C in 0.15 M NaCl solution (Table 1) agree relatively well with those reported in the literature [27] (20°C and 0.1 M KCl) indicating that the interaction of *c*-cdta with the Na(I) and K(I) ions is negligible. The *t*-cdta ligand behaves differently, since its $\log K_1^H$ value in 0.15 M KNO_3 is much higher (11.70) than in 0.15 M NaCl (9.54), because the stability constant of the $[Na(t\text{-cdta})]^{2-}$ complex is relatively high (log K_{NaL} = 4.4) [27], while the interaction of the ligand with K(I) ion is very week. The different behaviour of the two ligands indicates that the coordination

cage formed by the two iminodiacetate (ida) groups of the *c*-cdta is too small to accommodate the larger M(I) metal ions, while in the case of *t*-cdta the coordination cage is larger, where even a Na(I) ion can enter.

The stability constant of the Mg(II)- and $[Ca(c\text{-cdta})]^{2-}$ complexes obtained in this work are comparable with those, published in the literature (Table 1). For the *c*-cdta complexes of Mn(II), Zn(II) and Cu(II) there are not any stability constant data in literature. The stability constants of complexes formed with the *c*-cdta, *t*-cdta and edta ligands in 0.15 M NaCl (Table 1) do not differ considerable, because the formation of $[Na(t\text{-cdta})]^{2-}$ complex. Considering the formation of Na(I) complexes, it is more correct to compare the log K_{ML} values of the *c*-cdta with those log K_{ML} values which were obtained for the *t*-cdta complexes at 0.1 M KCl ionic strength. This comparison shows that the stability constants of the $[M(c\text{-cdta})]^{2-}$ complexes are lower by 2-3 log units than those of the $[M(t\text{-cdta})]^{2-}$ complexes (Table 1). These differences in the stability constants are related to the different size of the coordination cages formed by the donor atoms of the two ligands. ^{1}H-NMR studies indicated that the two ida groups in *t*-cdta occupy equatorial position [30] and this is probable for the case of the *c*-cdta, too. The distance between the two *N* atoms is significantly larger and so the coordination cavity is also larger for the *t*-cdta, in which the accommodation of metal ions of different size is more probable. The narrower size of the coordination cage in the *c*-cdta results in the stretching of the ligand structure by the entrance of a metal ion that leads to the lower stability constant.

The paramagnetic metal ions used as a component of the MRI CAs result in high proton relaxation rates. Since the free metal ions are toxic, their complexes are used as CAs. The longitudinal relaxation rate of water protons ($1/T_1$) in the presence of Mn^{2+} ions is significantly higher than in the presence of $[Mn(c\text{-cdta})]^{2-}$ or $[Mn(t\text{-cdta})]^{2-}$. (T_1 is the longitudinal relaxation time.) The relaxation effect of paramagnetic ions and complexes are expressed by their relaxivity values. The relaxivity (r_1, $mM^{-1}s^{-1}$) is the increase in the water proton relaxation rate resulted in by 1.0 mM increase in the concentration of the paramagnetic species. The relaxivity of the Mn(II).aq ion at 25°C and 20 MHz is 7.94 $mM^{-1}s^{-1}$, while that of the $[Mn(c\text{-cdta})]^{2-}$ complex is 3.85 $mM^{-1}s^{-1}$. This latter r_1 value is similar to that of the $[Mn(edta)]^{2-}$ (3.23 $mM^{-1}s^{-1}$) and $[Mn(t\text{-cdta})]^{2-}$ (3.62 $mM^{-1}s^{-1}$) complexes, in which one water molecule is coordinated in the inner sphere of the Mn(II).

The formation of [Mn(*c*-cdta)]$^{2-}$ complexes could be followed by measuring the water proton relaxation rates in equilibrium solutions of 1.0 mM Mn(II) and 1.0 mM *c*-cdta as a function of pH. At pH<2 only Mn(II).aq is present, when the $1/T_1$ values are high (Fig. 2). With the increase of pH, MnHL and MnL complexes are formed, when the water molecules are displaced from the inner sphere of Mn^{2+} ion and the proton relaxation rates decrease. After the formation of [Mn(L)] complex is complete (at about pH>5) the $1/T_1$ values are constant (this constant $1/T_1$ value is the relaxivity of the MnL complex). In Figure 2 the species distribution curves (calculated from the equilibrium data) are also presented (together with the $1/T_1$ values), calculated for the 1.0 mM Mn(II) - 1.0 mM *c*-cdta system. The data in Figure 2 indicate that the decrease of the proton relaxation rates with the increase of the pH occurs parallel with the formation of the MnHL and MnL complexes. The good agreement in the trend of the data obtained by pH-potentiometry and relaxometry, indicates the reliability of the equilibrium data.

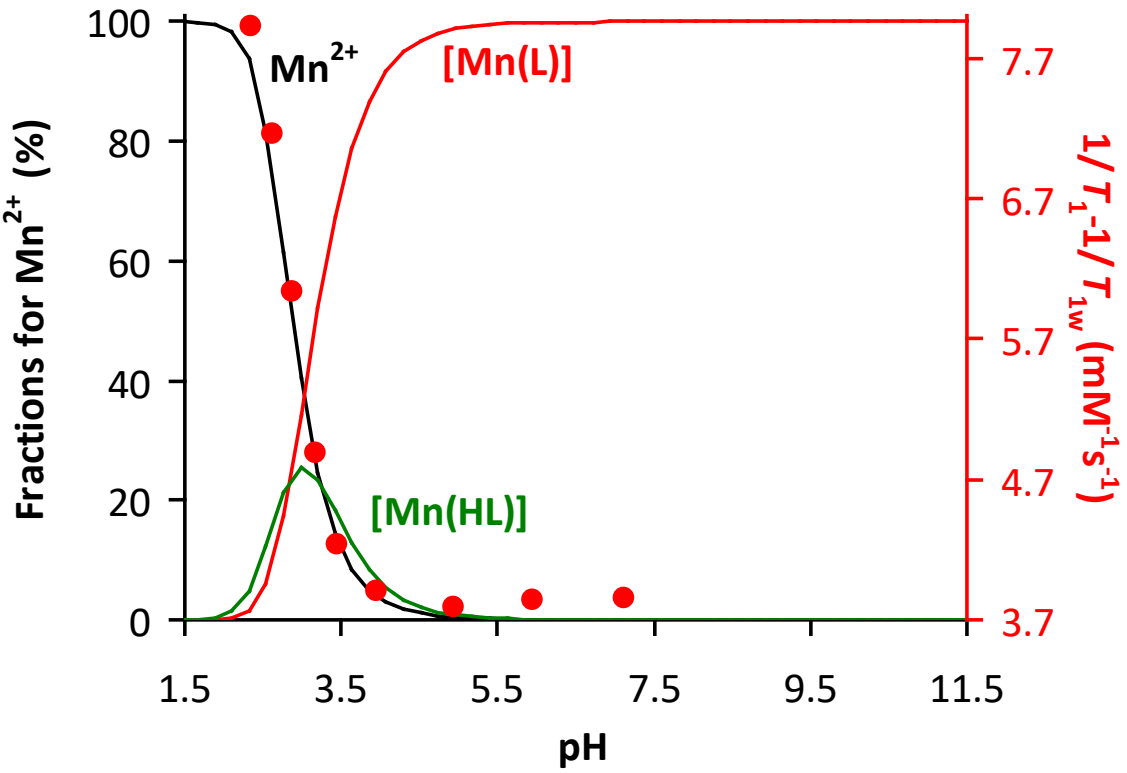

Figure 2. Species distribution curves and the relaxation rate ($1/T_1$-$1/T_{1w}$) profile (red points) of 1.021 mM [Mn(*c*-cdta)]$^{2-}$ as a function of pH (T = 25 °C, I=0.15 M NaCl, 20 MHz).

As it was underlined several times in the literature reliable stability data for Cu(II) – APC complexes can be obtained either by competition method with the use of auxiliary ligand (the equilibrium of the Cu(II) – auxiliary ligand system must be well known), or it can be accessed by using multiple methods simultaneously (e.g. UV-vis spectrophotometry applicable also in very acidic conditions and pH-potentiometry) [31]. The absorption spectra of the $[Cu(c\text{-cdta})]^{2-}$ complex as a function of H^+ ion concentration is shown on Figure 3. The spectrophotometric data were fitted simultaneously with the pH-potentimetric titration data and the stability constants determined are shown in Table 1. In line with the equilibrium data obtained for other metal ions studied, the stability constant of the $[Cu(c\text{-cdta})]^{2-}$ complex is smaller than the value of the corresponding $[Cu(t\text{-cdta})]^{2-}$ complex determined under identical conditions (the difference is ca. 0.7 log units).

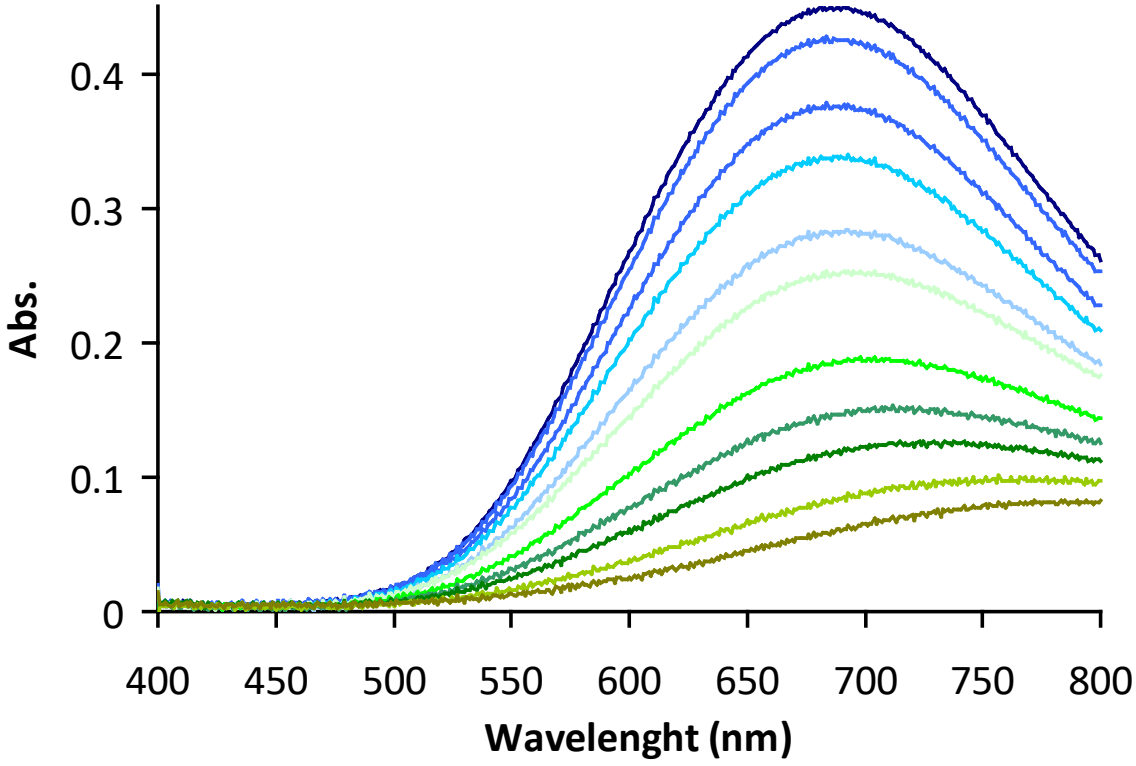

Figure 3. Absorption spectra of the $[Cu(c\text{-cdta})]^{2-}$ system as a function of $[H^+]$. Conditions: $[c\text{-cdta}^{4-}]$ = 3.528 mM, [Cu(II)] = 3.410 mM, 25 °C, 1.0 M $(Na^+ + H^+)Cl^-$, c_{H+} in the samples are as follows: 12.1; 18.8; 33.9; 49.0; 75.9; 101.0; 156.8; 205.0; 253.3; 349.8 and 462.4 mM (from top to bottom).

Dissociation kinetics of $[Mn(c\text{-cdta})]^{2-}$ complex

The fate of the MRI CAs in biological fluids is strongly influenced by their kinetic inertness, that is an important property in determining the extent of dissociation of the complex while in the body. For the Gd(III)-based CAs it was generally assumed that the deposition of Gd in the body was the result of the dissociation of Gd(III) complexes, that occurred through transmetallation reactions with the endogenous metal ions like Zn(II), Cu(II) and Ca(II) [33, 34]. To obtain information about the kinetic properties of CAs, the rates of the metal-exchange reactions are generally studied between the Gd(III) or Mn(II) complex and an exchanging metal ion, that is very often Cu(II), because in this case the reaction can easily be followed by spectrophotometry. The kinetic behaviour of $[Mn(c\text{-cdta})]^{2-}$ was studied similarly by following the exchange reactions depicted in Equation (4):

$$[Mn(c\text{-cdta})]^{2-} + Cu(II) \rightleftharpoons [Cu(c\text{-cdta})]^{2-} + Mn(II) \qquad \text{(eqn. 4)}$$

Since the stability constant of $[Cu(c\text{-cdta})]^{2-}$ is much higher than that of $[Mn(c\text{-cdta})]^{2-}$ (Table 1), reaction (4) takes place to completeness in the presence of Cu(II) excess (10-40 fold of Cu(II) excess was used). Under such conditions the reactions can be treated as pseudo-first-order ones kinetically. The rate of the exchange reaction (4) is directly proportional to the concentration of the complex and can be expressed as follows:

$$-\frac{\mathrm{d}[Mn(L)]_t}{\mathrm{d}t} = k_{obs}[Mn(L)]_t \qquad \text{(eqn. 5)}$$

In Equation (5) k_{obs} is a pseudo-first-order rate constant, $[Mn(L)]_t$ is the total concentration of complexes containing the $[Mn(c\text{-cdta})]^{2-}$ species. The rates of the exchange reactions (4) have been studied at four different Cu(II) concentrations in the pH range 4.03 – 5.03. The k_{obs} values obtained are shown in Figure 3.

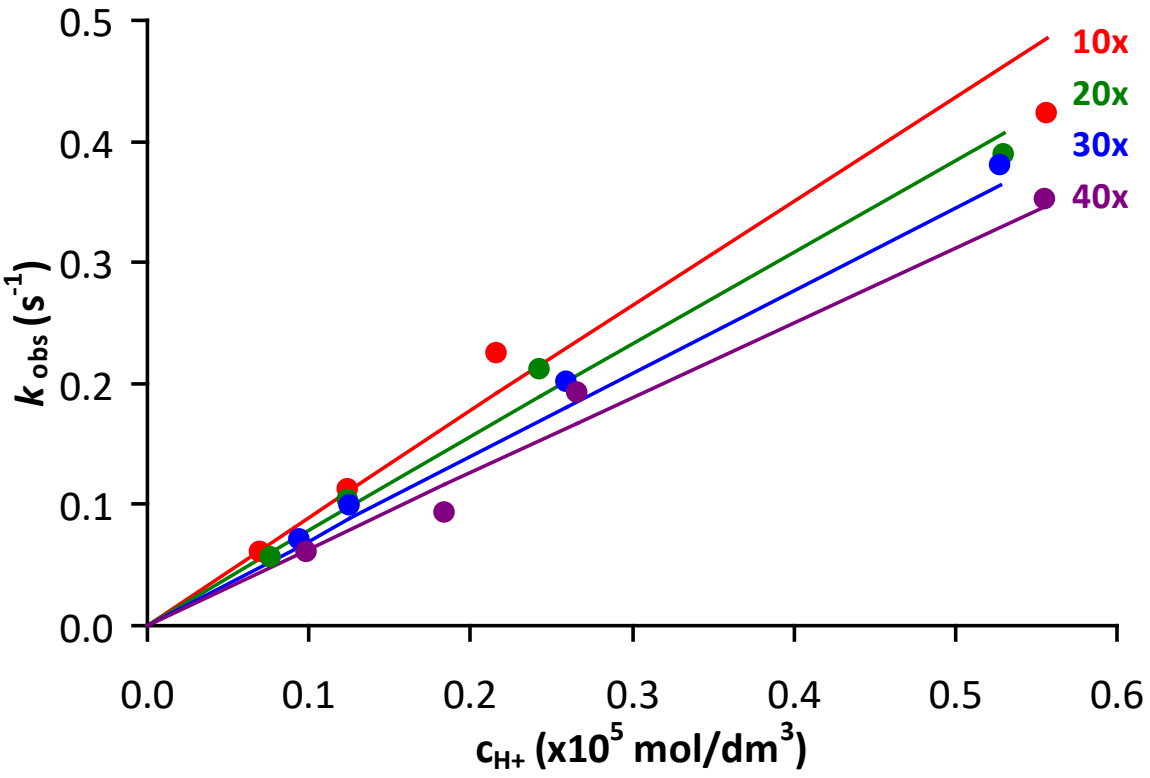

Figure 4. The rate constants (k_{obs}) characterizing the exchange reactions of [Mn(*c*-cdta)]$^{2-}$ (0.4 mM) with Cu(II) measured by stopped-flow method. The Cu(II) concentration are 4.0 mM (red), 8.0 mM (green), 12.0 mM (blue) and 16.0 mM (wine-red) (25°C, 0.15 M NaCl).

The observation of rate data in Figure 4 reveal that the k_{obs} values are directly proportional to the [H$^+$], that is the exchange reactions show first-order dependence on the H$^+$ ion concentration. The dependence of the k_{obs} values on the Cu(II) concentration is surprising, because the increase in the Cu(II) concentration results in a slight decrease in the reaction rates, that is the Cu(II) ions depress the rate of the exchange reactions. Similar phenomena were observed previously for the reaction of [Mn(*t*-cdta)]$^{2-}$ with Cu(II) and for the reactions between [Cd(*t*-cdta)]$^{2-}$ and Pb(II) or Cu(II) ions [18, 35]. The effect of the Cu(II) ions on the reaction rates can be interpreted by the formation of dinuclear [Mn(*c-cdta*)Cu] complexes, where presumably one acetate group of [Mn(*c*-cdta)]$^{2-}$ is coordinated to the Cu(II) ion and so the probability of protonation decreases (in fact [Mn(*c*-cdta)Cu] is a "dead-end" complex.) Since the reaction rate does not increase with the increase of the Cu(II) concentration, the exchange reactions do not take place with the direct attack of the Cu(II) ion. On the basis of the experimental data we came to the conclusion, that the exchange reactions between the

[Mn(*c*-cdta)]$^{2-}$ and Cu(II) ion occur through dissociation mechanism. After the rate determining dissociation of the complex, the released *c*-cdta ligand rapidly react with the Cu(II) ions by the formation of [Cu(*c*-cdta)]$^{2-}$. The dissociation of the [Mn(*c*-cdta)]$^{2-}$ complex can take place spontaneously and by the assistance of H^+ ions. The spontaneous dissociation is presumably very slow, while the proton assisted dissociation occurs relatively rapidly at pH values around 4-5. The protonation of [Mn(*c*-cdta)]$^{2-}$ presumable occurs at a carboxylate group (log K_{MHL} = 2.85), but for the dissociation of the complex the proton must be transferred to a N atom, when the protonated iminodiacetate (ida) group is not coordinated anymore and this intermediate may dissociate (or the complex may be re-formed by the dissociation of the proton). Considering the possible reaction pathways, the rate of dissociation of the complex can be expressed by Equation (6)

$$-\frac{[\mathrm{Mn(L)}]_t}{\mathrm{d}t} = k_0 + [\mathrm{Mn(L)}] + k_{\mathrm{MnHL}}[\mathrm{Mn(HL)}] \qquad \text{(eqn. 6)}$$

where k_0 and k_{MnHL} are the rate constants, characterizing the dissociation of the MnL and MnHL complexes, respectively.

Comparing the total concentration of the complex [Mn(*c*-cdta)]$^{2-}$ ([Mn(L)]$_t$ = [Mn(L)] + [Mn(HL)] + [Mn(L)Cu]), Equation (5) and (6), for the k_{obs} value Equation (7) is obtained:

$$k_{\mathrm{obs}} = \frac{k_0 + k_{\mathrm{MnHL}} \cdot K_{\mathrm{MnHL}} \cdot [\mathrm{H}^+]}{1 + K_{\mathrm{MnHL}}[\mathrm{H}^+] + K_{\mathrm{MnLCu}}[\mathrm{Cu}^{2+}]} \qquad \text{(eqn. 7)}$$

The term K_{MnHL} [H^+] in the denominator of Equation (7) is very small in the pH range 4.03 – 5.03, so it can be neglected. For the calculation of the unknown parameters Equation (7) has been used as follows:

$$k_{\mathrm{obs}} = \frac{k_0 + k_1 \cdot [\mathrm{H}^+]}{1 + K_{\mathrm{MnLCu}}[\mathrm{Cu}^{2+}]} \qquad \text{(eqn. 8)}$$

where $k_1 = k_{MnHL} K_{MnHL}$.

By fitting the k_{obs} values presented in Figure 4 to Equation (8) the k_0, k_1 and K_{MnLCu} values have been calculated and presented in Table 2. The k_0 value is very low, so it can be neglected.

Table 2. Rate and equilibrium constants characterizing the dissociation rates of the [Mn(*c*-cdta)]$^{2-}$, [Mn(*t*-cdta)]$^{2-}$ and [Mn(edta)]$^{2-}$ complexes.

	***c*-cdta**	*t*-cdta[a,b]	edta[a,b]
k_1 ($M^{-1}s^{-1}$)	**$(1.02\pm0.09)\times10^5$**	4.0×10^2	5.2×10^4
k_2 ($M^{-2}s^{-1}$)	**–**	**–**	2.3×10^8
k_3 ($M^{-1}s^{-1}$)	**–**	**–**	45±8
log K_{MnLCu}	**79±23**	79	**–**
log K_H	**2.85[c]**	2.90[c]	2.65[c]
$t_{1/2}$[d] (h)	**0.47**	12	0.076

[a] Ref [18]; [b] for [Mn(*t*-cdta)]$^{2-}$ $k_1 = 3.2\times10^2$ $M^{-1}s^{-1}$ and $t_{1/2}$ = 15 h while for [Mn(edta)]$^{2-}$ $k_3 = 3.0\times10^{-1}$ $M^{-1}s^{-1}$, $k_4 = \sim4.8\times10^1$ $M^{-2}s^{-1}$ and log K_{MnHL} =3.10 were found in Ref. [36]; [c] determined by pH-potentiometry and fixed in the data fitting; [d] calculated at pH = 7.4 in the presence of $c_{Cu2+} = 1\times10^{-5}$ M.

In Table 2, the k_1 rate constants and K_{MnLCu} stability constants obtained for the [Mn(*c*-cdta)]$^{2-}$ complex are compared with those of the [Mn(*t*-cdta)]$^{2-}$. The presented data indicate that the k_1 dissociation rate constant of [Mn(*c*-cdta)]$^{2-}$ is approximately 250 times higher than that of [Mn(*t*-cdta)]$^{2-}$. This difference is shown in the values of the half-life of dissociation, that is much longer for complex [Mn(*t*-cdta)]$^{2-}$. The results of these studies indicate that the kinetic inertness of the Mn(II) complex formed with the *c*-cdta isomer is significantly lower than that of the *t*-cdta isomer.

^{17}O and NMRD measurements

The nuclear magnetic relaxation dispersion (NMRD) profile of the [Mn(*c*-cdta)]$^{2-}$ was measured at three different temperatures (298, 310 and 323 K) in the frequency range 0.01-80

MHz to gain information on the relaxation properties of the complex (Figure 5). The NMRD profiles show a single dispersion at 1-10 MHz which is typical of low molecular weight Mn^{2+} complexes. Their temperature dependence indicates that the relaxivity of the complex is limited by fast rotation. Several physico-chemical parameters affect the relaxivity of a paramagnetic metal complex, such as the water exchange rate, the electron spin relaxation parameters and the rotational correlation time. The temperature dependence of the transverse and longitudinal ^{17}O relaxation rates can provide information on the water exchange rate (k_{ex}) and the rotational correlation time (τ_R), respectively, while the chemical shift is related to the number of the water molecules directly coordinated to the paramagnetic metal center (q). Variable temperature transverse and longitudinal relaxation rates and chemical shifts were measured for an aqueous solution of $[Mn(c\text{-cdta})]^{2-}$ and for a diamagnetic reference at 9.4 T. The T_1 values showed negligible difference between the Mn(II) complex and the reference, thus were not included in the calculations. The reduced ^{17}O transverse relaxation rates, $1/T_{2r}$ and chemical shifts, $\Delta\omega_r$, have been fitted according to the Swift-Connick equations, by assuming a simple exponential behaviour for the electron spin relaxation. The water exchange rate, k_{ex}^{298}, its activation enthalpy, $\Delta H^{\neq}$, and $1/T_{1e}^{298}$ were calculated (the activation energy of electron spin relaxation was fixed to 1 kJ/mol). The hydration number was fixed to q=1 based on analogy to $[Mn(t\text{-cdta})]^{2-}$ and on the relaxivity value measured at 20 MHz (r_1=3.85 $mM^{-1}s^{-1}$, $r_{1,[Mn(t\text{-cdta})]2-}$=3.62 [18]). To characterize the rotational dynamics of the complex, the ^1H NMRD data were analyzed by the Solomon-Bloembergen-Morgan (SMB) [37] and Freed models [38] (inner- (IS) and outer-sphere (OS) relaxation mechanisms) and the Swift-Connick [39, 40] equations related to the solvent exchange (see Supporting Information). The parameters for water exchange were fixed to those determined from the ^{17}O NMR study. The distances between the metal ion and the inner and outer sphere water protons were also fixed (r_{MnH} = 2.83 Å and a_{MnH} = 3.6 Å), as well as the diffusion coefficient and its activation energy ($D_{MnH} = 26 \times 10^{-10}$ m^2s^{-1} and E_{MnH} = 18 kJ/mol^{-1}) and the activation energy of the modulation of the zero-field-splitting (E_v = 1.0 kJ/mol). The values of the electron relaxation parameters τ_v^{298} and Δ^2 were found to be 7.6±0.9 ps and $(4.1\pm0.8)\times10^{20}$ s^{-2}, respectively. The best-fit parameters obtained are given in Table 3 and compared with those of $[Mn(t\text{-cdta})]^{2-}$ and $[Mn(4\text{-het-cdta})]^{2-}$ complexes [41, 42]. The experimental data and the fitted curves are shown in Figures 5 and 6.

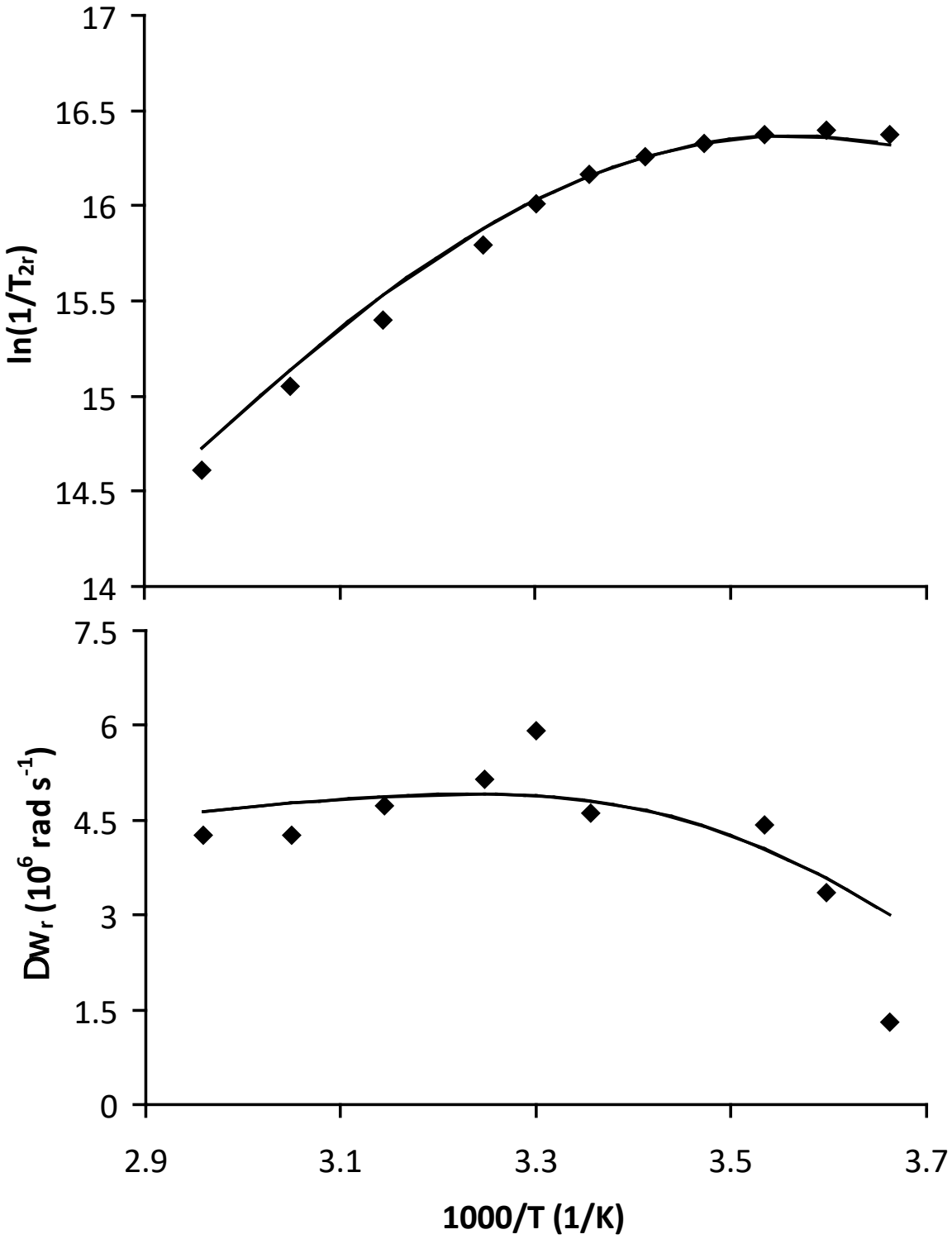

Figure 5. Variable temperature reduced transverse ^{17}O relaxation rates (top) and chemical shifts (bottom) recorded for $[Mn(c\text{-cdta})]^{2-}$ (B = 9.4 T). The solid lines correspond to the fit of the data.

Table 3. Parameters obtained from the analysis of ^{17}O NMR and ^{1}H NMRD data for the $[Mn(c\text{-cdta})(H_2O)]^{2-}$ complex.

Parameter	[Mn(*c*-cdta)]$^{2-}$	[Mn(*t*-cdta)]$^{2-}$ [c]	[Mn(4-het-cdta)]$^{2-}$ [d]
k_{ex}^{298} (x10^7 s^{-1}) [a]	22.5 ± 0.5	14.0	17.6
$\Delta H^{\ddagger}$ (kJ mol^{-1}) [a]	42.0 ± 0.8	42.5	36.2
$\Delta S^{\ddagger}$ (J K^{-1} mol^{-1}) [a]	+56 ± 4	–	–
$A_O/\hbar$ (10^6 rad s^{-1}) [a]	42.7 ± 0.9	4.2	40
$1/T_{1e}^{298}$ (x10^7/ s^{-1}) [a]	27.0 ± 0.5	0.65	7
E_{rH} (kJ mol^{-1}) [b]	21.8 ± 2.0	–	26.2
τ_{rH}^{298} (ps) [b]	52 ± 5	–	104.9

[a] from ^{17}O NMR; [b] from NMRD; [c] Ref. [41]; [d] Ref. [42].

As Figure 5. shows, the reduced transverse ^{17}O relaxation rates undergo a changeover at ~290 K between the fast and intermediate water exchange regime. Importantly, the water exchange rate has a significant contribution in the overall correlation time ($1/\tau_c = k_{ex} + 1/T_{1e}$; k_{ex} varying from 10 to 80% in the temperature range 273-338 K) which makes possible to accurately determine k_{ex}. The k_{ex}^{298} value characterizing the water exchange of [Mn(*c*-cdta)]$^{2-}$ is ca. 60% higher than that of [Mn(*t*-cdta)]$^{2-}$, which can be likely related to the structural differences between the two complexes. The smaller coordination cage of the *cis* derivative induces more steric crowding around the metal ion. The importance of steric crowding to accelerate water exchange has been previously demonstrated in the case of a dissociatively activated mechanism [43]. The high positive activation entropy points to a dissociative mechanism, thus the [Mn(*c*-cdta)]$^{2-}$ complex can be expected to have a faster water exchange, as it is indeed observed.

On the other hand, k_{ex}^{298} is the half of the value determined for [Mn(edta)]$^{2-}$ (47.1×10^7 s^{-1}) [44]. This is related to the more rigid structure of the cdta^{4-} ligands which detains the rearrangement of the coordination environment during the water exchange process. The water exchange is also several times slower on [Mn(*c*-cdta)]$^{2-}$ than on the 1,4-do2a or do1a complexes, having a very different, macrocyclic structure [45]. The rotational correlation time (τ_{rH}^{298}) obtained from the analysis of the relaxivity data is in the usual order of magnitude of typical low molecular weight complexes.

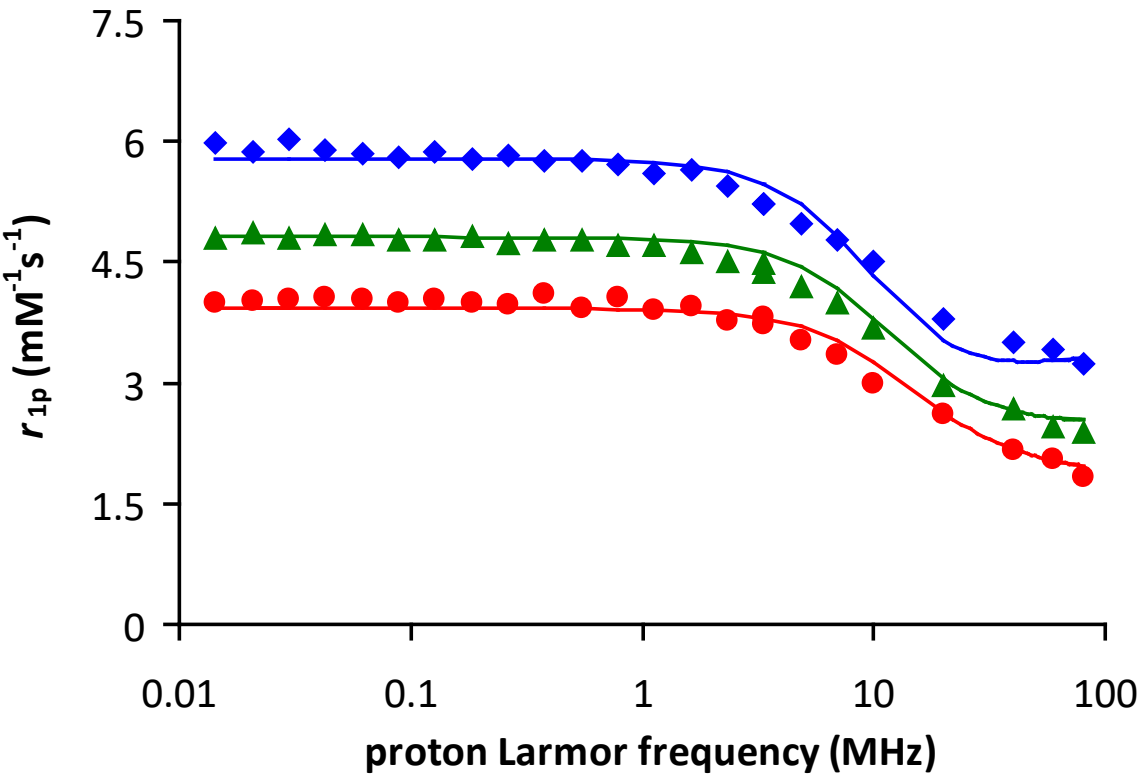

Figure 6. ^{1}H NMRD profiles of [Mn(*c*-cdta)]$^{2-}$ at 25 °C (♦), 37 °C (▲) and 50 °C (●).

Summary

Our efforts to find suitable ligand for Mn(II) complexation started from equilibrium, kinetic and relaxometric characterization of Mn(II) complexes formed with commercially available open-chain ligands a few years ago [18]. The studies performed revealed that the rigid *t*-cdta forms relatively inert complex with Mn(II) ion (the half-life of the dissociation is expected to be 12 hours near to physiological conditions). However, to best of our knowledge Mn(II) complexes of other rigid edta derivative ligands such as *cis*-1,2-cyclohexanediamine or *o*-phenylenediamine tetraacetates (e.g. *c*-cdta or phdta) were not studied in detail in this respect. The distance between the two nitrogen atoms of the ida groups in these ligands are expected to differ substantially form that in *t*-cdta (where it is accepted to be 4 Å) and so the coordination properties of the ligands are likely to be affected by this structural diversity.

The thermodynamic, kinetic (solvent and dissociation kinetic data) and relaxation parameters expressed in terms of water exchanges rates and relaxivity values (at 25 °C) are collected in the following table. The data collected for these hexadentate chelators indeed indicate that the Mn(II) complexes of these ligands differ notably. The most pronounced difference is seen for the dissociation kinetic data as the Mn(II) complex formed by the *cis*-derivative ligand shows properties similar to those seen for other labile complexes of linear

edta-type ligands [18] whereas the *t*-cdta forms relatively inert Mn(II) complex. Moreover, the stability (especially the conditional stability) behaves alike by making the *trans*-1,2-cyclohexanediamine unit to be an excellent "building block" when tailoring inert Mn(II) complexes for safe MRI applications.

Table 4. Comparison of the most important physico-chemical data of the Mn(II) complexes formed with *t*-cdta and *c*-cdta ligands.

Parameter	$[Mn(c\text{-cdta})]^{2-}$	$[Mn(t\text{-cdta})]^{2-}$ [a]
$\log K_{[Mn(L)]}$	14.19	14.32
pMn[b]	7.82	8.68
$t_{1/2}$ (h)[c]	0.47	12
k_{ex}^{298} ($x10^7$ s^{-1})	22.5	14.0[d]
r_{1p}^{298} [e]	3.85	3.62

[a] Ref. [18]; [b] pMn values were calculated at pH=7.4 by using 0.01 mM Mn(II) and ligand concentration as suggested by É. Tóth and co-workers [29]; [c] the half-lives (h) of dissociation were extrapolated to pH=7.4 by using 0.01 mM Cu(II) ion concentration; [d] form Ref. [41]; [e] at 25 °C and 20 MHz.

Experimental section

Synthesis

All commercially purchased reagents (Sigma-Aldrich) and solvents (Scharlab) were used as received and without further purification. NMR spectra were acquired on Bruker Avance 360 and 400 MHz spectrometers and processed/analyzed using MestreNova 8.1 (Mestrelab Research) or Topspin (Bruker) softwares. The ESI QTOF (Electro Spray Ionization Quadrupole Time of Flight) spectrometry was performed at the Department of Applied Chemistry of the University of Debrecen.

a). Synthesis of *cis*-1,2-CDTA-tetraethyl ester: Ethyl-bromoacetate (6.14 g, 36.8 mmol, 4.2 equiv.) was dissolved in dry acetonitrile and added dropwise to the mixture of 1.00 g (8.76 mmol) *cis*-1,2-diaminocyclohexane, 5.66 g N,N-diisopropylethylamine (43.8 mmol, 5.0 equiv.) and 1.31 g (8.76 mmol, 1.0 equiv.) of NaI prepared in dry acetonitrile (30 ml). The reaction mixture was then heated to reflux in N_2 atmosphere and kept at this temperature for 7 hours. The precipitate formed in the course of reaction was filtered off from the hot solution and the filtrate was evaporated under reduced pressure. The resulting oily residue was

dissolved in 40 mL of bi-distilled water and extracted with portions of chloroform (3×40 mL). The combined organic fraction was dried over anhydrous Na_2SO_4 and evaporated under reduced pressure. The purification of the title product by flash chromatograpy on silica gel by using petrolether and ethyl acetate (increasing the ethyl acetate content of the eluent gradually form 10:1 to 5:1 by volume) yielded the pure substance (0.82 g which corresponds to 20 % yield). R_f in 5:1 petrolether : ethyl acetate is 0.38.

^{1}H-NMR: (360.13 MHz, $CDCl_3$): δ = 1.23 (12H, t, *J* = 7.11 Hz, -O-CH_2-C**H$_3$**); 1,29 (2H, m, -C**H$_2$**-); 1.43 (2H, m, -C**H$_2$**-); 1.62 (2H, m, -C**H$_2$**-); 1.79 (2H, m, -C**H$_2$**-); 3.16 (2H, d, *J* = 6.88 Hz, -C**H**-); 3.70 and 3.79 (8H, AB doublet, $^2J_{AB}$ = 17.90 Hz, -N-C**H$_2$**-COO-); 4.11 (8H, q, *J* = 7.11 Hz, -O-C**H$_2$**-CH_3). ^{13}C-NMR: (90.55 MHz, $CDCl_3$): δ = 14.34 (4C, s, -O-CH_2-**C**H_3); 23.44 (2C, s, -**C**H_2-**C**H_2-); 26.88 (2C, s, -**C**H_2-); 53.08 (4C, s, -N-C**H$_2$**-COO-); 60.27 (4C, s, -O-**C**H_2-CH_3); 60.55 (2C, s, -**C**H-); 172.58 (-N-CH_2-**C**OO-). MS (ESI-Q-TOF): *m/z* [M+] calculated for $C_{22}H_{38}N_2ONa$: 481.252; found: 481.251

b). Synthesis of *cis*-1,2-CDTA: 0.40 g NaOH (10 mmol, 6 equiv.) was dissolved in 1,0 mL of bi-distilled water and was added portionwise to the solution of 0.75 g (1.64 mmol) *cis*-1,2-CDTA-tetraethyl ester dissolved in 15 mL of ethanol. The reaction mixture was heated to 78 ◦C and refluxed at this temperature for 24 h. The white precipitate formed during the reaction (Na_4(c-cdta)) in the reaction mixture was filtered off and washed twice with cold ethanol (2×10 mL), diethyl ether (2×10 mL) and dried to constant weight. The solid obtained was dissolved in minimal amount of water required to dissolve it (3.0 mL) and pH of the sample was set to pH=2.02 by addition of concentrated HCl. The white precipitate formed as a result of acid addition was filtered off and washed with small portions of acidified distilled water (pH=2.50), cold ethanol (2×5 mL), diethyl ether (2×5 mL) and dried until the weight of the product become constant. Yield: 0.22 g (39 %).

^{1}H-NMR: (360.13 MHz, D_2O): δ = 1,51 (2H, m, -C**H$_2$**-); 1.74 (2H, m, -C**H$_2$**-); 1.83 (2H, m, -C**H$_2$**-); 2.00 (2H, m, -C**H$_2$**-); 3.51 (2H, m, -C**H**-); 3.83 and 4.01 (8H, AB doublet, $^2J_{AB}$ = 17.39 Hz, -N-C**H$_2$**-COO-). ^{13}C-NMR: (90.55 MHz, D_2O): δ = 22.11 (2C, s, -**C**H_2-**C**H_2-); 23.19 (2C, s, -**C**H_2-); 54.76 (4C, s, -N-C**H$_2$**-COO-); 61.26 (2C, s, -**C**H-); 172.81 (-N-CH_2-**C**OO-). MS (ESI-Q-TOF): *m/z* [M+] calculated for $C_{14}H_{21}N_2O_8NaNa$: 391.109; found: 391.109

Equilibrium studies

The chemicals (MCl_2 salts) used in the studies were of the highest analytical grade. The concentration of the stock solutions was determined by complexometric titration using a standardized Na_2H_2edta solution and appropriate indicators (Patton & Reeder ($CaCl_2$), Eriochrome Black T ($MgCl_2$ and $MnCl_2$), xylenol orange ($ZnCl_2$), murexid ($CuCl_2$)) [46].

The pH-potentiometric titrations were carried out with a Methrohm 888 Titrando titration workstation, using a Metrohm 6.0233.100 combined electrode. The titrated solutions (6.00 mL) were thermostated at 25 °C. The samples were stirred and kept under inert gas atmosphere (N_2) to avoid the effect of CO_2. The calibration of the electrode was performed by two point calibration (KH-phthalate (pH = 4.005) and borax (pH = 9.177) buffers). The calculation of $[H^+]$ from the measured pH values was performed with the use of the method proposed by Irving *et al*. [47] by titrating a 0.01 M HCl solution (I = 0.15 M NaCl) with a standardized NaOH solution. The differences between the measured (pH_{read}) and calculated pH (-log $[H^+]$) values were used to obtain the equilibrium H^+ concentrations from the pH-data obtained in the titrations. The ion product of water was determined from the same experiment in the pH range 11.4 – 12.0.

The concentration of the *c*-cdta ligand was determined by pH-potentiometric titration, comparing the titration curves obtained in the presence and absence of moderate Mn(II) excess. The protonation constants of *c*-cdta as well as the stability and protonation constants of the complexes formed with Mg(II) Ca(II), Mn(II), Cu(II) and Zn(II) were also determined by pH-potentiometric titration. The metal-to-ligand concentration ratio was 1:1 (the concentration of the ligand was generally 2.50 – 3.00 mM). The pH-potentiometric titrations curves were measured in the pH range 1.8 – 11.8 and 44 – 205 mL NaOH–pH data pairs were collected and fitted.

The stability constant and solution speciation of the $[Mn(c\text{-cdta})]^{2-}$ complex was confirmed using ^1H relaxometry in order to support the stability constant value obtained by pH-potentiometry (for details about T_1 measurements, see the "Relaxivity determination" section below). 3.00 mL of a 1.02 mM $[Mn(c\text{-cdta})]^{2-}$ sample were titrated with solid NaOH or gasous HCl (in order to avoid sample dilution) to adjust the pH in the range 1.97 – 7.12, followed by recording and averaging of 5 – 6 T_1 values for each pH data point.

Owing to the high conditional stability of $[Cu(c\text{-cdta})]^{2-}$, the formation of the complex was complete (nearly 100%) even at pH = 1.54 (starting point of the pH-potentiometric titration). For this reason, 12 out-of-cell (batch) samples containing a slight excess of ligand and the Cu(II) ion were prepared (c_L = 3.528 mM, c_{Cu2+} = 3.410 mM, 25 °C, 0.5 M

(Na^++H^+)Cl^-). The samples, whose acidity was varied in the concentration range of 12.1 – 462 mM, were equilibrated for 1 day before recording the absorption spectra at 25 °C in Peltier thermostated semi-micro 1 cm Hellma® cells using a Varian CARY 1E, UV-Vis spectrophotometer. The molar absorptivity of the [Cu(*c*-cdta)]$^{2-}$, complex was determined at 21 wavelengths (600 – 800 nm range) by recording the spectra of 1.72×10^{-3}, 2.55×10^{-3} and 3.48×10^{-3} M complex solutions, while for the Cu(II) ion, previously published molar absorptivity values (determined under identical conditions) [48] were used for the data fitting. The molar absorption coefficients of monoprotonated [CuH(*c*-cdta)]$^{2-}$ were calculated during the simultaneous data refinement (UV-vis and pH-potentiometric titration curves). The protonation (ligand and complexes) and stability constants (complexes) were calculated from the titration data with the PSEQUAD program [49].

Kinetic studies

The dissociation rates of the [Mn(*c*-cdta)]$^{2-}$ chelate were studied at 25 °C (Peltier thermostated) and 0.15 M NaCl ionic strength by stopped-flow method monitoring the formation of the Cu(II) complex at 300 nm using an Applied Photophysics DX-17MV instrument. All dissociation reactions were performed under pseudo-first order conditions where the exchanging metal ion (Cu(II)) was in 10–40-fold excess relative to the complex ($c_{complex}$ = 2.0×10^{-4} M, pH range 4.25–5.10). The kinetic studies were carried out in a non-coordinating buffer to maintain the pH in the samples constant (0.05 M *N*,-methylpiperazine (nmp) with log K_2^H = 4.34 under the conditions applied). The pseudo-first-order rate constants (k_{obs}) were calculated by fitting the absorbance-time data series to equation 9:

$$A_t = (A_0 - A_e)e^{-k_{obs}t} + A_e \qquad \text{(eqn. 9)}$$

where A_t, A_0 and A_e are the absorbance at time t, at the start and at the equilibrium of the reaction, respectively. The calculations were performed with the computer program Micromath Scientist, version 2.0 (Salt Lake City, UT, USA) by using a standard least-squares procedure [50].

^{1}H-, and ^{17}O-NMR relaxometry

Longitudinal ($1/T_1$) and transverse ($1/T_2$) relaxation rates and chemical shifts of an aqueous solution of the Mn(II) complex (pH=7.4, 10.3 mM) and of a diamagnetic reference ($HClO_4$ acidified water, pH = 3.3) were measured in the temperature range 273 – 338 K using

a Bruker Avance 400 (9.4 T, 54.2 MHz) spectrometer. The temperature was determined according to previous calibration by means of ethylene glycol and methanol as standards [51]. $1/T_1$ and $1/T_2$ values were determined by the inversion - recovery and the Carr – Purcell – Meiboom –Gill spin – echo technique, respectively [52]. The technique of the ^{17}O NMR measurements has been described previously [53]. To avoid susceptibility corrections of the chemical shifts, a glass sphere fitted into an 10 mm NMR tube was used to contain the samples. To improve sensitivity, ^{17}O enriched water (10% $H_2{}^{17}O$, CortecNet) was added to the solutions to reach around 1% enrichment.

Proton NMRD profiles of the $[Mn(c\text{-cdta})]^{2-}$ complex (1.00 mM, pH = 7.4) were recorded in aqueous solution on a Stelar SMARTracer Fast Field Cycling relaxometer (0.01 − 10 MHz) and a Bruker WP80 NMR electromagnet adapted to variable field measurements (20 − 80 MHz) and controlled by a SMARTracer PC-NMR console. The temperature was monitored by a VTC91 temperature control unit and maintained by a gas flow. The temperature was determined by previous calibration with a Pt resistance temperature probe. The least-squares fit of the ^{17}O NMR and of the NMRD data was performed using Visualiseur/Optimiseur [54, 55] running on a MATLAB 8.3.0 (R2014a) platform.

Relaxivity determination

The longitudinal water proton relaxation rate ($r_1 = 1/T_1 - 1/T_w$) was measured at 20 MHz with a Bruker Minispec MQ-20 relaxometer (Bruker Biospin, Germany). Samples were thermostated by using a circulating water bath at 25.0 ± 0.2 ºC. The longitudinal relaxation times (T_1) were measured by using the inversion recovery method ($180^o - \tau - 90^o$) by averaging 5 – 6 data points for each concentration point obtained by using 14 different τ values (τ values ranging between 0 to at least 6 times the expected T_1).

Abbreviations

MRI	Magnetic resonance imaging
APC	aminopolycarboxylate
CA	Contrast Agent

dtpa	Diethylenetriaminepentaacetic acid
dota	1,4,7,10-Tetraazacyclododecane-1,4,7,10-tetraacetic acid
NSF	Nephrogenic Systemic Fibrosis
edta	Ethylenediaminetetraacetic acid
trans-1,2-cdta	*trans*-1,2-Diaminocyclohexane-N,N,N′,N′-tetraacetic acid
cis-1,2-cdta	*cis*-1,2-Diaminocyclohexane-N,N,N′,N′-tetraacetic acid
DIPEA	N,N-diisopropylethylamine
ida	Iminodiacetate
NMRD	Nuclear magnetic relaxation dispersion
4-het-cdta	4-((1-(2-Hydroxyethyl)-1H[1,2,3]triazol-4-yl)methoxy)methyl-trans-1,2-diaminocyclohexane-N,N,N',N'-tetraacetic acid
1,4-do2a	1,4,7,10-Tetraazacyclododecane-1,4-diacetic acid
do1a	1,4,7,10-Tetraazacyclododecane-1-acetic acid
phdta	*o*-Phenylenediamine tetraacetate
ESI QTOF	Electro Spray Ionization Quadrupole Time of Flight
nmp	*N*-methylpiperazine

Appendix A. Supplementary data

Supplementary data associated with this article (^{1}H-, ^{13}C-NMR and MS data of the pure compounds, and the equations related to the solvent exchange kinetics data refinement) can be found, in the online version, at http://dx.doi.org/10.1016/xxxxxxxxxxxxxxxxx .

Acknowledgements

This research was funded by the Hungarian Scientific Research Fund (OTKA K-120224 project), Le Studium, Loire Valley Institute for Advanced Studies (Gy.T. and F.K.K.) and the János Bolyai Research Scholarship (Gy.T. and F.K.K.) of the Hungarian Academy of

Sciences. E. T. acknowledges support of the Ligue contre le Cancer (France). The research was also supported by the EU and co-financed by the European Regional Development Fund under the project GINOP-2.3.2-15-2016-00008.

References

[1] Anderson L. J., Welch M. J., Chem. Rev. 1999, 99(9), 2219-34.

[2] Stimmel J.B., Kull F.C. Jr., Nucl. Med. Biol. 1998, 25, 117-125.

[3] Nayak T. K., Brechbiel M. W., Bioconjug. Chem. 2009, 20(5), 825-841.

[4] Parker D., Dickins R. S., Puschmann H., Crossland C. and Howard J. A. K., Chem. Rev. 2002, 102 (6), 1977-2010.

[5] Montgomery C. P., Murray B. S., New E. J., Pal R., Parker D., Acc. Chem. Res., 2009, 42 (7), 925-937.

[6] Caravan P., Ellison J. J., McMurry T. J., Lauffer R. B., Chem. Rev. 1999, 99(9), 2293-2352.

[7] The Chemistry of Contrast Agents in Medical Magnetic Resonance Imaging, 2nd edition, Eds. Merbach A. E, Helm L. Tóth É., John Wiley and Sons, London, 2013.

[8] Grobner T., Nephrol. Dial. Transplant. 2006, 21, 1104-1108.

[9] Marckmann P., Skov L., Rossen K., Dupont A., Damholt M. B., Heaf J. G., Thomsen H. S., J. Am. Soc. Nephrol. 2006, 17, 2359-2362.

[10] Kitajima K., Maeda T., Watanabe S., Ueno Y., Sugimura K., Int. J. Urol. 2012, 19, 806-811.

[11] Kanda T., Fukusato T., Matsuda M., Toyoda K., Oba H., Kotoku J., Haruyama T., Kitajima K., Furui S., Radiology 2015, 276, 228-232.

[12] Kanal E., Tweedle, M. F., Radiology 2015, 275, 630-634.

[13] Roberts D. R., Lindhorst S. M., Welsh C. T., Maravilla K. R., Herring M. N., Braun K. A., Thiers B. H., Davis W. C., Invest Radiol. 2016, 51(5), 280-289.

[14] Birka M., Wentker K. S., Lusmöller E., Arheilger B., Wehe C. A., Sperling M., Stadler R., Karst U., Anal. Chem. 2015, 87(6), 3321-8.

[15] Troughton J. S., Greenfield M. T., Greenwood J. M., Dumas S., Wiethoff A. J., Wang J., Spiller M., McMurry T. J., Caravan P. Inorg. Chem., 2004, 43(20), 6313-23

[16] Wang S., Westmoreland D. T., Inorg. Chem. 2009, 48(2), 719-27.

[17] Drahoš B., Kubíček V., Bonnet C. S., Hermann P., Lukeš I, Tóth É., Dalton Trans. 2011, 40(9), 1945-51.

[18] Kálmán F. K., Tircsó Gy., Inorg. Chem. 2012, 51(19), 10065-17.

[19] Drahos B., Kotek J., Hermann P., Lukes I., Tóth É., Inorg. Chem. 2010, 49, 3224-38.

[20] Tei L., Gugliotta G., Fekete M., Kálmán F. K., Botta M., Dalton Trans. 2011, 40(9), 2025-32

[21] Regueiro-Figueroa M., Rolla G. A., Esteban-Gómez D., de Blas A., Rodríguez-Blas T., Botta M., Platas-Iglesias C., Chem. Eur. J. 2014, 52(20), 17300–17305.

[22] Gale E. M., Atanasova I. P., Blasi F., Ay I., Caravan P., J. Am. Chem. Soc. 2015, 137, 15548-15557.

[23] Forgács A., Pujales-Paradela R., Regueiro-Figueroa M., Valencia L., Esteban-Gómez D., Botta M., Platas-Iglesias C., Dalton Trans. 2017, 46, 1546-1558.

[24] Phukan B., Patel A. B., Mukherjee C., Dalton Trans. 2015, 44, 12990-12994.

[25] Ussov W.Y., Beljanin M.L. Borodin O.Y., Churin A.A., Bezlepkin A.I., Filimonov V.D., Medical Visualization (in russian) 2009, 5 121-132.

[26] Ussov W.Y., Bogunetsky A.A., Babokin V.E., Belyanin M.L., Goltsov S.G., Filimonov V.D., Tomsk/RU In ECR, 2014 March 6–10, 2014, Vienna, Austria; B-0904.

[27] Critical Stability Constants, Ed. Martell A. E., Smith R. M., Vol. 1-6. Plenum Press, New York, London, 1974-1989.

[28] Charlier L., Merciny E., Fuger, J., Anal. Chim. Acta, 1985, 178, 299-306.

[29] Drahoš B., Kotek J., Hermann P., Lukeš I., Tóth É., Inorg. Chem. 2010, 49(7), 3224-3238

[30] Sudmeier J. L., Reilley C. N., Anal. Chem. 1964, 36(9), 1707-712.

[31] Regueiro-Figueroa M., Ruscsák E., Fra L., Tircsó Gy., Tóth I., de Blas A., Rodríguez-Blas T., Platas-Iglesias C. and Esteban-Gómez D., Eur. J. Inorg. Chem. 2014, 36, 6165-6173.

[32] Rodríguez-Rodríguez A., Garda Z., Ruscsák E., Esteban-Gómez D., de Blas A., Rodríguez-Blas T., Lima L. M. P., Beyler M., Tripier R., Tircsó Gy.. Platas-Iglesias C., Dalton Trans., 2015,44, 5017-5031.

[33] Thakral C., Abraham J.L., J. Cutan Pathol. 2009, 36(12),1244-54.

[34] Port M., Idée J.M., Medina C., Robic C., Sabatou M., Corot C., Biometals. 2008, 21(4), 469-90.

[35] Smith G. F., Margerum D. W, Inorg. Chem. 1969, 8(1), 135-138.

[36] Margerum D. W., JPausch. B., Nyssen G. A., Smith G. F., Anal. Chem. 1969, 41(2), 233-238.

[37] Bloembergen N.; Morgan L. O., J. Chem. Phys. 1961, 34, 842-850.

[38] Freed J. H., J.Chem.Phys. 1978, 68, 4034-4037.

[39] Swift T. J., Connick R. E., J.Chem.Phys. 1962, 37, 307-320.

[40] Swift T. J., Connick R. E., J.Chem.Phys. 1964, 41, 2553-2554.

[41] Maguit J., Meier R., Zahl A., Eldik R., Inorg. Chem. 2008, 47, 5702-5719.

[42] Vanasschen C., Molnár E., Tircsó Gy., Kálmán F. K., Tóth É., Coenen H. H., Neumaier B., manuscript submitted for publication to Inorg. Chem.

[43] Ruloff R., Tóth É., Scopelliti R., Tripier R., Handle H., Merbach A. E., Chem. Commun. 2002, 22, 2630-2631.

[44] Esteban-Gomez D., Cassino C., Botta M., Platas-Iglesias C., RSC Advances 2014, 4, 7094-7103.

[45] Rolla G. A., Platas-Iglesias C., Botta M., Tei L., Helm L., Inorg. Chem., 2013, 52, 3268-3279.

[46] Schwarzenbach G., Flaschka H. A., Complexometric titrations. Barnes & Noble: 1969.

[47] Irving H. M., Miles M. G., Pettit L. D., Anal. Chim. Acta 1967, 38, 475-488.

[48] Molnár E., Camus N., Patinec V., Rolla G. A., Botta M., Tircsó Gy., Kálmán F. K., Fodor T., Tripier R., Platas-Iglesias C., Inorg. Chem. 2014, 53 (10), 5136-5149.

[49] Zékány, L.; Nagypál, I., PSEQUAD. In Computational Methods for the Determination of Formation Constants, Leggett, D. J., Ed. Springer US: Boston, MA, 1985; pp 291-353.

[50] https://www.micromath.com/ (last accessed on 30th of April, 2017).

[51] Raiford D. S., Fisk C. L., Becker E. D., Anal. Chem. 1979, 51, 2050-51.

[52] Meiboom S., Gill D., Rev. Sci. Instrum. 1958, 29, 688-691.

[53] Micskei K., Helm L., Brucher E., Merbach A. E., Inorg. Chem., 1993, 32, 3844-3850.

[54] Yerly F., VISUALISEUR 3.3.7; Lausanne, Switzerland, 2006.

[55] Yerly F., OPTIMISEUR 3.3.7. Lausanne, Switzerland, 2006.

Highlights

- Stability constants, water exchange rates and the relaxivities of the isomeric $[Mn(cdta)]^{2-}$ complexes are similar

-The conditional stability and the inertness of the $[Mn(t\text{-}cdta)]^{2-}$ is higher than that of $[Mn(c\text{-}cdta)]^{2-}$

-The *trans*-1,2-cyclohexanediamine unit is an excellent “building block” when designing Mn(II) complexes as safe MRI agents

TOC graphic

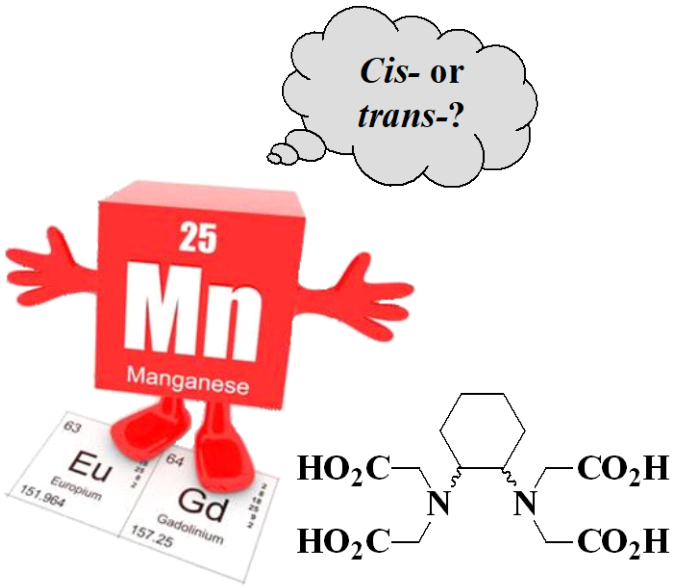

M(II) complexes formed with *c*-cdta (*cis*-1,2-diaminocyclohexane-*N,N,N′,N′*-tetraacetic acid). chelator have been investigated by pH-potentiometry, UV-vis spectrophotometry, ^{1}H and ^{17}O NMR relaxometry. pMn as well as the inertness of the Mn(II) complex formed with *c*-cdta ligand were found to differ substantially form those found for the *trans*- derivative while the water exchange rate and the relaxivity do not differ remarkably. Our results confirm, that the *t*-cdta platform has better potential for further ligand development owing to better dissociation kinetic parameters of its Mn(II) complex.